

Measurement of high dynamic range luminance according to video signal(E_R , E_G , E_B) using a fish-eye lens

*Yasuo Nagai *Takaharu Miyoshi **Xueying Qin
Katsumi Tadamura *Eihachiro Nakamae

*Hiroshima Institute of technology ** Zhejiang University
Yamaguchi University *Sanei Co.LTD

Abstract For the color design on an outdoor industrial product, it is requested to the computer graphics creating their models not only their shapes but also the match of color to the background photographs or each frame image of the video sequence. For that, the high dynamic range luminance corresponding to not the achromatic luminance signal but individual video signal (E_R , E_G , E_B) is necessary. In this paper, we propose how to take a picture and calibrate to acquire all skylight luminance distribution according to the (E_R , E_G , E_B) signal by using a digital camera with fish-eye lens and ND filters.

Keyword: color design, measurement of skylight luminance distribution, direct incident sunlight, video signal, luminance signal

1. Introduction

For color designing of an outdoor industrial product, it is necessary to keep of optical balance of its model and the background photograph or each frame of the video sequence to say nothing its shape.

In this paper, we propose how to promptly measure all sky luminance distribution with highly accurate high dynamic range (HDR) according to video signal (E_R , E_G , E_B) of which ratio is guaranteed for different chromaticity of each pixel.

After the HDR technique ([1]), using achromatic luminance signals of plural photographs taken by several shutter speeds and stops, by which a wide radiance signal is restored had been proposed, a lot of papers related to the HDR have been presented. For instance, photographing the reflected light with a high-speed shutter camera by setting up a mirror ball at the position of a rendering model ([2],[3]), the technique using the stereo images with two fisheye lens cameras and generating the patch for an environmental optical mapping ([4]), and the discussions on the influence of vignette and infrared rays sensitivity and the spectrum penetration characteristics of ND filters ([5]). However, these all handle luminance signal E_Y of black and white, deal only with the saturation area of this signal, and do not consider the error due to the signal of each chromaticity; i.e., the saturation and the lower bound of individual video signal (E_R , E_G , E_B). Moreover, the measuring range uses neither saturation value for the direct sunlight.

The standard skylight luminance distributions to fine weather and complete cloudy weather of CIE (International Commission on Illumination) ([6],[7]) are used for

making the montages and synthetic videos of outdoor scenes in daytime (e.g. refer to [8]). And, there are models corresponding to all weathers containing the intermediate average sky (e.g. refer to [9],[10]).

These measurements, however, target only the luminance distribution of skylight and exclude intensity of direct sunlight, and do not have chromaticity information on the skylight. Though reference [11] measures the luminance and color temperature of skylight and obtains their correlation coefficient statistically, the problem is expensive and cannot correspond to the skylight distribution in the locale photograph. Thus, for photographing skylight, it is demanded that a simple data acquisition method with portability, which can correspond to the change of the luminance distribution of the light sources due to the weather conditions.

In this paper, we use the ND filters together with a digital camera wearing the fisheye lens, and propose a highly accurate measurement and calibration method for all skylight luminance distribution with information of video signal (E_R , E_G , E_B). The next section describes how to calibrate the luminance meter according to video signal (E_R , E_G , E_B), and in section 3 we propose a handy photograph of the skylight luminance in all azimuths including direct incident sunlight according to (E_R , E_G , E_B), and show its effectiveness. Finally, we give the summary and some future problems.

2. Video Signal(E_R , E_G , E_B) and Luminance L_Y

We verify the calibration method and accuracy of the proposed luminance meter according to video signal (E_R , E_G , E_B) with a color digital camera on the market by using the light sources of two kinds of radiance distribution and four kinds of targets.

2.1 Luminance Signal E_Y and Luminance L_Y

To consider the relations of video signal (E_R , E_G , E_B), achromatic color luminance signal E_Y , and luminance L_Y [cd/m^2], the following combinations are measured. Light sources: a metal halide lamp (4,000K) and a fluorescent lamp (6,300K); Target: the standard white paper of CIERGB color specification; White balance: “Preset” which revises the color balance with the standard white paper before photograph, and “Sun” which is the solar light and “Auto” which automatically sets suitable shutter speed S (k); the latter two are prepared in a popular digital camera in the market;

here E_Y and L_Y are the studio standard of the NTSC as shown by the next equation,

$$E_Y = 0.299E_R + 0.587E_G + 0.114E_B. \quad (1)$$

Hereafter, value L_Y of the luminance meter is assumed to be true value.

Let us discuss by using typical examples of combination mentioned above.

2.1.1 Color temperature of light source and luminance signal of light

Fig. 1(a) shows relations of luminance signal E_Y with luminance L_Y on the metal halide lamp and the fluorescent lamp, and the standard white paper is used. Both values E_Y of the metal halide lamp and fluorescent lamp are all most the same, and it

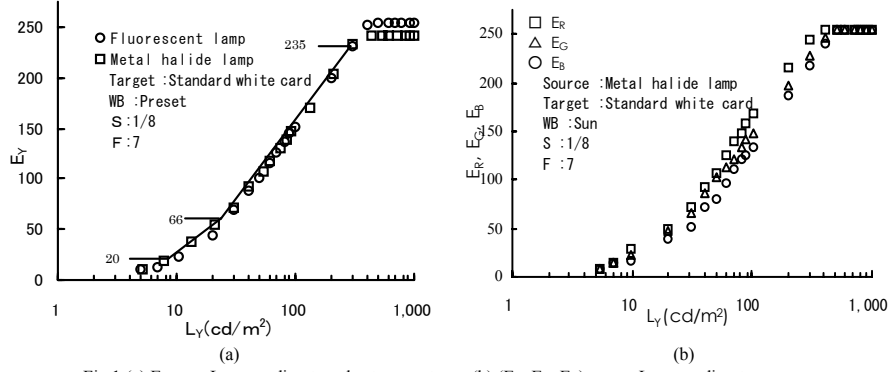


Fig 1 (a) E_Y vs. L_Y according to color temperature : (b) (E_R, E_G, E_B) vs. L_Y according to white balance: Sun

can closely resemble the quality, in two broken lines facing with the L_Y [cd/m^2] of the logarithmic scale. That is, it is possible to express by the next equations by using equation (1),

$$\begin{aligned} L_{Y1} &= 11.2e^{0.0144E_Y} & (E_{Y1\max}(235) > E_Y \geq E_{Y1\min}(66)) \\ L_{Y2} &= 5.24e^{0.0254E_Y} & (E_{Y2\max}(66) > E_Y > E_{Y2\min}(20)) \end{aligned} \quad (2)$$

In this system, the coverage to the luminance meter is set from 20 to 235 levels, because as for the image signal in case of achromatic color digital inscription of 8 [bit], black and 100 [%] levels are set to 16 and 235 levels, respectively.

2.1.2 White balance and luminance signal E_Y

Because of adjusting the white balance in advance, the broken lines of “Preset” are $E_R = E_G = E_B$ for any L_Y , and in case of “Sun”, the broken lines of three signals consist of 3 sections, keeping $E_R > E_G > E_B$, and in parallel (refer to Fig. 1(b));

that is, “Preset” and “Sun” show that they are effective for measuring highly accurate luminance L_C guaranteed color ratio (E_R, E_G, E_B) of the target at least which is close to white within the range of $(E_{Y1\max} > (E_R \cup E_G \cup E_B) \geq E_{Y2\min})$ by revising with the coefficients of broken lines in the figures.

In general the broken lines of E_Y vs. L_Y of “Preset” and “Sun” differ depending upon the camera, but they do not change with photograph condition.

On the other hand, in case of “Auto”, the characteristic curves change at the time of each photograph condition. Thus, it should be avoided to use for background photographs.

2.2 Chromaticity of Target and Luminance L_Y

In order to verify different chromaticity of target influences onto the characteristics of L_Y vs. (E_R, E_G, E_B) , we use the targets of blue, white, green and red.

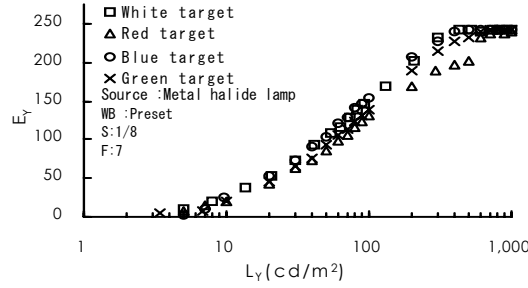


Fig. 2 E_Y vs. L_Y according to color of targets

2.2.1 Achromatic luminance L_Y vs. luminance signal E_Y for different chromaticity of target

As shown in Fig. 2, the difference of L_Y between blue and white targets is extremely small. On the other hand, the difference L_Y between red and white reaches 2.5 times at 200. We discuss those causes and measures in the next paragraph.

2.2.2 Luminance L_C according to video signal (E_R , E_G , E_B) of which ratio is guaranteed for different chromaticity

Fig. 3(a) and (b) show the relations of L_Y vs. (E_R , E_G , E_B) for the targets with green and red.

- When the measurement condition is “Preset” and a white paper target, the relations of L_C vs. (E_R , E_G , E_B) has $E_R=E_G=E_B$; thus, the full range of the measurement can be secured.
- Signal of (E_R , E_G , E_B) corresponding to L_C , by which a blue color is guaranteed, does not influence L_Y too much, because the percentage contribution to E_Y of E_B is only 11 [%] (refer to equation (1)).
- As shown in Fig. 3(a), a parallel region of signal curves (E_R , E_G , E_B) corresponding to L_C , by which chromaticity value of green, is guaranteed is from 60 [cd/m^2] to 200 [cd/m^2], and $L_{YG} \approx L_C$. However, it is necessary to deal with careful each (E_R , E_G , E_B) for other ranges.

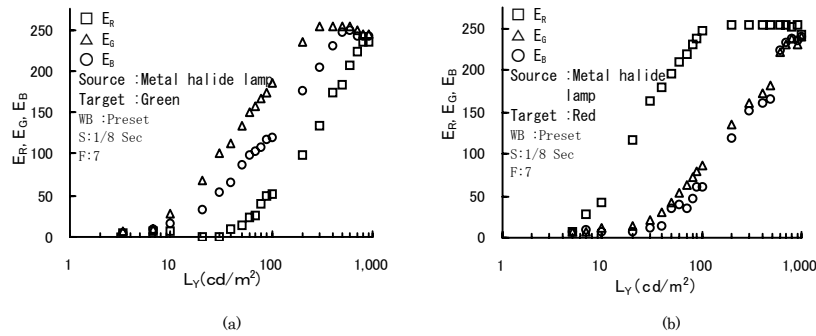


Fig. 3 (E_R , E_G , E_B) vs. L_Y according to each color of target

- d) As shown in Fig. 3(b), the parallel region of signal curves (E_R , E_G , E_B) corresponding to L_C , by which chromaticity value of red is guaranteed, is from 50 [cd/m^2] to 90 [cd/m^2]. The influence of E_G is large even over the upper limit because the contribution rate to E_Y of E_R is 30[%]. This causes large error of L_C outside coverage in Fig. 2.
- e) c) and d) show that the regions of each curve of signals are influenced by chromaticity of illuminated surfaces. As for the chromaticity of the source of light, similar measures are necessary, even though we omit the discussions because of space.

2.3 Luminance measurement of distributed incident skylight

Under the different weather conditions such as fine or cloudy daylight and/or at different time such as sunrise and sunset, the luminance distribution of incident sunlight and skylight and their color are much different. The more higher chromaticity of light sources and larger reflections, the more coverage of video signal becomes narrow. Therefore, it is desired to photograph by selecting an appropriate combinations of shutter speed $S(s)$, stop $F(f)$ and ND filter $ND(d)$; and get luminance L_C according to (E_R , E_G , E_B) within the coverage approximated by equations (2). The following algorithm gives accurate luminance for chromaticity value of (E_R , E_G , E_B) at any pixel, $X(i)(i=1, 2, \dots, n), Y(j)(j=1, 2, \dots, m)$ in each frame.

Expressing the luminance under the condition of $M(k=1)$ at pixel, $X(i), Y(j)$, as $L_{C1}(i,j)$, the relationship between luminance $L_{Ck}(i,j)$ and ($E_R(i,j)$, $E_G(i,j)$, $E_B(i,j)$) can be expressed by the following equation;

$$L_{Ck}(i,j) = M(k) * L_{C1}(i,j), \quad (3)$$

where $M(k)(i=1,2,\dots,k,\dots,k_m)$ is the stored array of magnifications in which exposure is calculated for each image with the combination of $S(s)$, $F(f)$ and $ND(d)$.

3. Whole Skylight Luminance Distribution Meter Guaranteed on Signal Ratio (E_R , E_G , E_B)

The following points can be enumerated as the problems to photograph whole skylight luminance distribution guaranteed on signal ratio (E_R , E_G , E_B) promptly and in high accuracy.

- Direct incident sunlight of the zenith onto the ground at fine weather is quite large; over $10^9[\text{cd}/\text{m}^2]$. Direct sunlight at the complete blue sky reaches 85 [%] or more.
- The diameter of the sun is only 0.3 [%] comparing with that of fisheye lens used in this paper.
- It is necessary to establish how to photograph which considering about the effect of vignette, prism effect and distortion of the fisheye lens. Therefore, measurement accuracy of direct incident sunlight with chromaticity of whole skylight exerts a large

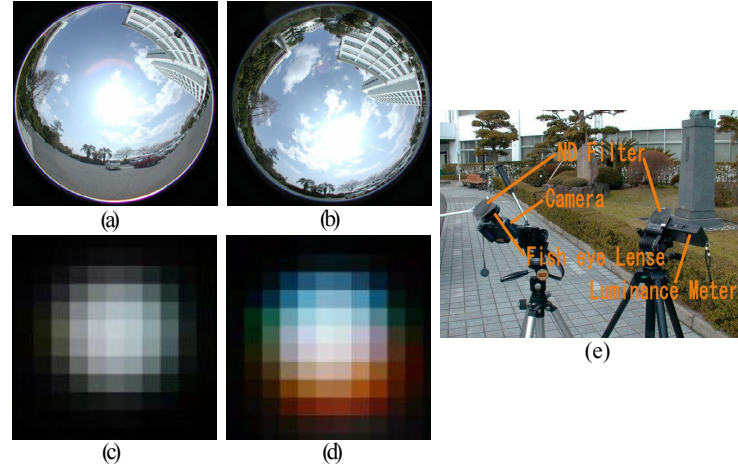


Fig. 4 Photographing skylight distribution:(a) and (b) distortions of fisheye lens; (c) and (d) effects of prism;(e) devices

influence on the rendering result for the color design.

In the next section, let us present how to calibrate the luminance meter to measure the whole skylight luminance distribution guaranteed on signal ratio (E_R , E_G and E_B).

3.1 Taking Photographs

By using one example, let us explain the outline of how to photograph.

- In order to briefly make plural photograph where exposure differs, some ND filters with handle are prepared, and photographed by covering the vicinity of the sun (Refer to Fig. 4(e)).
- In principle, “Preset” and “Sun” are used for white balance.
- In order to minimize the influences of vignette and distortion of the fisheye lens, and to avoid losing symmetric property of distribution of chromaticity due to prism effect, if the direct sunlight irradiates, the direction of camera should be set to the sun and opposite direction and at cloudy weather the camera should direct to the zenith and that of opposite direction because of the following reason.
 - a) When the angle between the center of lens and the sun is large, the geometric distortion occurs (refer to Fig. 4(a) and (b)).
 - b) The vignette of the fisheye lens is quite large (refer to Fig. 4(c) and (d)).

3.2 Luminance measurement of distributed incident skylight

The concept of the algorithm for setting the measured luminance on each pixel taken into account of video signal ($E_R(i,j)$, $E_G(i,j)$, $E_B(i,j)$) is as follows:

- a) In the followings, in order to explain concisely, let's take up the processing on the $L_{C1}(i,j)$ at pixel $X(i), Y(i)$. Every video signal ($E_R(i,j)$, $E_G(i,j)$, $E_B(i,j)$) existing in the characteristic curve L_{C1} , for exposure $M(k)$ shown by equation (3) belongs to one of the following cases;

$K(i,j)=0$: untreated pixel,

$K(i,j)=1$: over-exposure pixel,

$K(i,j)=2$: pixel within the region approximated by equation (2); highest accurate region,
 $K(i,j)=3$: pixel within the region approximated by equation (3); highly accurate region,
 $K(i,j)=4$: pixel with too high chromaticity value,
 $K(i,j)=5$: pixel with any of $(E_R(i,j), E_G(i,j), E_B(i,j))$ of over exposure and less than 25 for the case in $M(k+1)$,
 $K(i,j)=6$: too under-exposure pixel.
 b) Followings are the outline of the processing for calculating $L_{Ck}(i,j)$ in ascending order of $M(k)$ ($k=1, k, \dots, km$);
 step0: Set the range at $(E_{Y1max}=255) \geq E_Y \geq (E_{Y1min}=0)$ in equation (2), and at $(E_{Y1min}=66) > E_Y \geq (E_{Y2min}=0)$ in equation (3), respectively; $K(i,j) \leftarrow 0$; set $k=0$;
 step1: $M(k)=M(k+1)$;
 step2: $E_{max} = \max(E_R(i,j), E_G(i,j), E_B(i,j))$;
 step3: In case of $235 \geq E_{max} \geq 66$, $L_{Ck}(i,j) = \text{equation (2)}$;
 In case of $235 \geq ((E_R(i,j) \cap E_G(i,j) \cap E_B(i,j)) \geq 66$, $K(i,j) \leftarrow 2$; go to step 9;
 In case of $66 > ((E_R(i,j) \cup E_G(i,j) \cup E_B(i,j)))$, $K(i,j) \leftarrow 4$; go to step 9;
 step4: In case of $66 > E_{max} \geq 20$, $L_{Ck}(i,j) = \text{equation (3)}$;
 In case of $66 > ((E_R(i,j) \cap E_G(i,j) \cap E_B(i,j)) \geq 20$, $K(i,j) \leftarrow 3$; go to step 9;
 In case of $20 > ((E_R(i,j) \cup E_G(i,j) \cup E_B(i,j)))$, $K(i,j) \leftarrow 4$; go to step 9;
 step5: In case of $(k=1) \cap (20 \geq E_{max})$, $L_{Ck}(i,j) = \text{equation (3)}$; $K(i,j) \leftarrow 6$; go to step 9;
 Step6: In case of $(k \leq km) \cap (20 \geq E_{max})$; $M(k)=M(k-1)$; $L_{Ck}(i,j) = \text{equation (2)}$; $K(i,j) \leftarrow 5$; go to step 9;
 Step7: In case of $(k \neq km) \cap (E_{max} > 235)$, go to step 1;
 Step8: In case of $(k=km) \cap (E_{max} > 235)$, $L_{Ck}(i,j) = \text{equation (2)}$; $K(i,j) \leftarrow 1$; go to step 9;
 Step9: got to the next pixel;

After finishing the processing mentioned above for every pixel in the frame, the quality of the luminance distribution with video signal information can be evaluated as follows;

- The pixel with $K(i,j)=1$ indicates that its luminance is saturated. Thus, it is recommended to retake the photograph, if possible.
- The pixel with $K(i,j)=4$ indicates that its exposure is insufficient from the viewpoint of HDR. Thus, it is recommended to retake the photograph, if possible.
- The pixel with $K(i,j)=0$ indicates that as for the exposure of its pixel is at least insufficient from the viewpoint of HDR. Thus, it is recommended to interpolate with the pixels of its neighborhood.

3.3 Calibration of luminance meter for high intensity by measuring direct incident sunlight

The measurement solid angle of the luminance meter is $1[\text{deg}]$, beside the solid angle of the sun, $32[\text{min}]$. Because measurement value L_{YL} of the luminance meter is an average value, it is necessary to obtain luminance L_{Ysun} of the sun by using the measurement area S_L and the area S_s of the sun, that is, L_{Ysun} is obtained from the next equation,

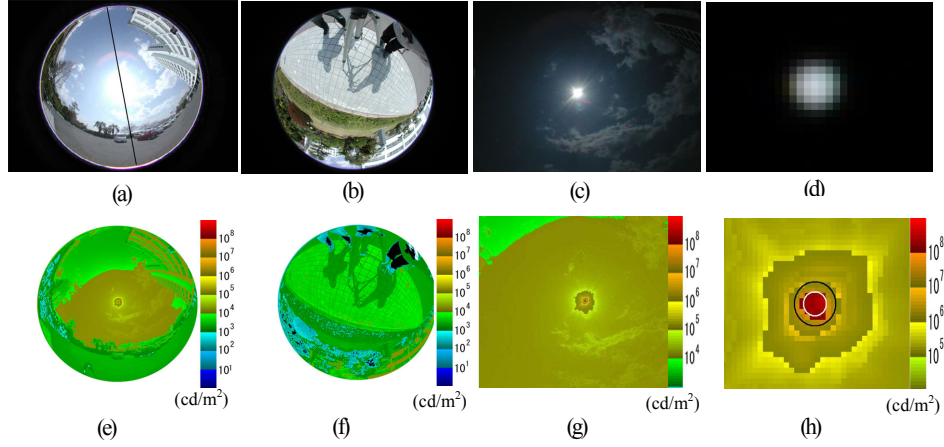


Fig. 5 Photographs of skylight and luminance distributions : (a) photograph facing the directions of the Sun ; (b) opposite side of (a) ; (c), (d) enlarged views of (a); from (e) to (h) luminance distributions of from (a) to (d)

$$L_{Ysun} = L_{YL} (S_S * L_{YS} + (S_L - S_S)L_{YC}) / S_S * L_{YS} \quad (4)$$

The luminance of the sunlight, L_{Ysun} , measured by the luminance meter is $2.89 \times 10^8 [\text{cd}/\text{m}^2]$. The luminance calculated by using the ratio of the inner and outer areas of the sun is $3.10 \times 10^8 [\text{cd}/\text{m}^2]$. That is, assuming that the former S_L is the true value, the error must be 7[%] or more.

3.4 Skylight measurement with simple luminance meter

Fig. 5 shows one example; skylight distribution was measured with the luminance meter after calibration mentioned above.

Fig. 5(a), (b), (c), and (d) show photographs and their expansion charts, and Fig. 5(e), (f), (g), and (h) the pseudo color charts of their luminance, respectively.

Fig. 6 shows the luminance distribution assumed that the numbers of photographs are half of the original ones; that is, the odd number photograph was used, and the difference between luminance of the proposed method and the case of Fig. 5(e), respectively. In these figures, the white area shows that the difference of both is zero.

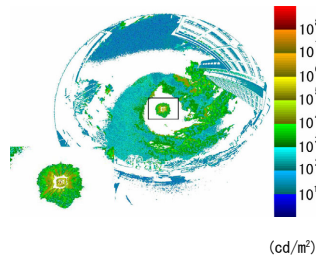


Fig. 6 Influence of number of photographs on luminance distribution accuracy (different luminance distribution with Fig5 (e): odd number photographs)

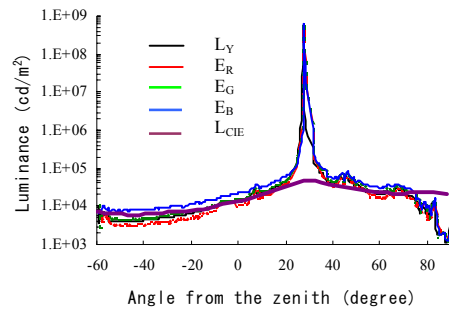


Fig. 7 Skylight luminance characteristic curves on straight line connecting the sun with zenith in Fig. 5 (a)

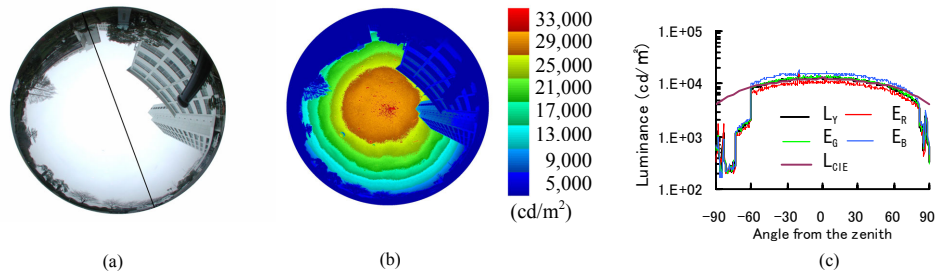


Fig.8 Skylight luminance distribution at thin cloudy weather: (a) photograph, (b) Luminance distribution of (a) (capitation), and (c) skylight luminance characteristic curves on straight line in Fig. (a)

Fig. 7 shows luminance L_C on the line through the sun and the zenith, distribution curves of each element of (E_R , E_G , E_B) in luminance L_C , and CIE-standard luminance distribution characteristic curve.

Fig. 8(a) shows a photograph in cloudy weather, and Fig. 8 (b), the luminance distribution, and Fig. 8(c), the luminance distribution on the line in Fig. 8(a). These figures depict that it is extremely effective so that the proposed luminance meter may measure the skylight luminance guaranteed chromaticity, quickly and accurately.

4. Summary and Problems in the Future

In this paper, we proposed how to promptly measure all sky luminance distribution with highly accurate and high dynamic range using fish-eye lens and ND filter in order to use for color design of outside industrial products, and showed its effectiveness, that is;

(a) How to take proper photographs quickly and accurately, in order to measure the whole sky luminance distribution with information of video signal (E_R , E_G , E_B); (b) Verifying the characteristics of the proposed luminance meter in laboratory experiment; (c) Calibrating the luminance meter for high luminance and wide range by measuring the direct incident sunlight; (d) How to avoid influences from vignette, distortion and prism effect of fisheye lens and displaying the usefulness by measuring skylight luminance distributions at fine and cloudy weather.

The following should be thought as the problems in the future.

- Making of application examples by the proposed measurement;
- Verifying the usefulness by using the scenes illuminated by neon signs and compound light sources with different colors such as at stages.

References

- [1] P. Debevec, J. Malik, "Recovering High Dynamic Range Radiance Maps from Photographs", Computer Graphics Proc., Annual Conference Series, pp.369-378, (1997)
- [2] P. Debevec, "Rendering Synthetic Objects into Real Scenes: Bridging Traditional and Image-based Graphics with Global Illumination and High Dynamic Range Photography", Computer Graphics Proc., Annual Conference Series, pp.189-198, (1998)
- [3] J. Unger, A. Wenger, T. Hawkins, A. Gardner, P. Debevec, "Capturing and Rendering with Incident Light Fields", Eurographics Symposium on Rendering 2003, pp.1-10, 2003

- [4] I. Sato, Y. Sato, K. Ikeuchi, "Acquiring a radiance onto a real scene", IEEE Trans. Visualization and Computer Graphics, Vol.5, No.1, pp. 1-12, (1999)
- [5] J. Stumpfel, A. Jones, A. Wenger, P. Debevec, "Direct HDR Capture of the Sun and Sky" 3rd International Conference on Virtual Reality, Computer Graphics, Visualization and Interaction in Africa, pp.132-138 (2004)
- [6] CIE "Natural daylight, Official recommendation, Compute Rendu CIE 13th Session, Committee" E-3.2, Vol. II, part 3-2 II-IV & 35-37 (1955)
- [7] CIE "Spatial distribution of daylight-Overcast sky and clear sky, Pub." CIE 003.2 (1994)
- [8] X. Qin, E. Nakamae, and K. Tadamura "Automatically Compositing Still Images and Landscape Video Sequences", IEEE Computer Graphics and Applications, January/February 2002, pp.68 - 78, (2002)
- [9] R. Perez, R. Seals, J. Michalsky "All-Weather Model for Sky Luminance Distribution – Preliminary Configuration and Validation", Solar Energy Vol.50. No. 3, pp.235-245, (1993)
- [10] N. Igawa, H. Nakamura, T. Matsuzawa, Y. Koga "All Sky Model as a Standard Sky Luminance Distribution – Part 2 A Numerical Expression of Sky Luminance Distributions for All Sky Conditions –", J. Light & Vis. Env., Vol. 27, No. 1, pp.16-26, (2003)
- [11] T. Takagi, H. Takaoka, T. Ohshima, Y. Ogata, "Accurate Rendering Technique Based on Colorimetric Conception", Computer Graphics, Vol.24, No.4, pp.263-272, (1990)